HHS Public Access

Author manuscript

Neurosci Lett. Author manuscript; available in PMC 2022 January 10.

Published in final edited form as:

Neurosci Lett. 2021 January 10; 741: 135502. doi:10.1016/j.neulet.2020.135502.

Morphine and HIV-1 Tat interact to cause region-specific hyperphosphorylation of tau in transgenic mice

Michael Ohene-Nyako[1], **Sara R. Nass**[1], **Yun K. Hahn**[2], **Pamela E. Knapp**[1,2,3], **Kurt F. Hauser**[1,2,3]

[1]Department of Pharmacology and Toxicology, Virginia Commonwealth University School of Medicine, Richmond, VA 23298, USA

[2]Department of Anatomy and Neurobiology, Virginia Commonwealth University School of Medicine, Richmond, VA 23298, USA

[3]Department of Insitute for Drug and Alcohol Studies, Virginia Commonwealth University School of Medicine, Richmond, VA 23298, USA

Abstract

Opiate abuse is prevalent among HIV-infected individuals and may exacerbate HIV-associated age-related neurocognitive disorders. However, the extent to which HIV and opiates converge to accelerate pathological traits indicative of brain aging remains unknown. The pathological phospho-isotypes of tau (pSer396, pSer404, pThr205, pSer202, and pThr181) and the tau kinases GSK3β and CDK5/p35 were explored in the striatum, hippocampus, and prefrontal cortex of inducible male and female HIV-1 Tat transgenic mice with some receiving escalating doses of morphine for 2 weeks. In the striatum of male mice, pSer396 was increased by co-exposure to morphine and Tat as compared to all other groups. Striatal pSer404 and pThr205 were increased by Tat alone, while pSer202 and pThr181 were unchanged. A comparison between Tat transgenic female and male mice revealed disparate outcomes for pThr205. No other sex-related changes to tau phosphorylation were observed. In the hippocampus, Tat increased pSer396, while other phosphorylation sites were unchanged and pSer202 was not detected. In the prefrontal cortex,

Corresponding Author (permanent address): Kurt F. Hauser, Ph.D., Pharmacology and Toxicology, Virginia Commonwealth University, Kontos Medical Sciences, Building, 1217 East Marshall Street, Richmond, Virginia 23298-0613, Phone: (804) 628-7579; Fax: (804) 828-0676, kurt.hauser@vcuhealth.org.

Author Contribution

Michael Ohene-Nyako: Conceptualization, Experimental design, Data curation and analyses, Manuscript writing- original draft, review and editing.

Sara R. Nass: Data curation, Manuscript writing- review and editing.

Yun Hahn: Resources, Manuscript review and editing.

Pamela E. Knapp: Experimental design, Funding acquisition, Manuscript writing- original draft, review and editing.

Kurt F. Hauser: Experimental design, Funding acquisition, Manuscript writing- original draft, review and editing.

Declaration of Conflict of Interest

The authors state they have no conflicts of interest.

Data Accessibility Statement

The authors confirm that all data pertaining to this manuscript are available and will be shared with the scientific community upon request.

morphine increased pSer396 levels, which was unaffected by Tat, while other phosphorylation sites were unaffected. Assessment of tau kinases revealed no changes to striatal GSK3β (phosphorylated or total) or the total CDK5 levels. Striatal levels of phosphorylated CDK5 and p35, the activator of CDK5, were increased by Tat and with morphine co-exposure, respectively. P35 levels positively correlated with those of pSer396 with Tat and morphine co-exposure. The results reveal region-specific hyperphosphorylation of tau induced by exposure to morphine, Tat, and unique morphine and Tat interactions.

Graphical Abstract

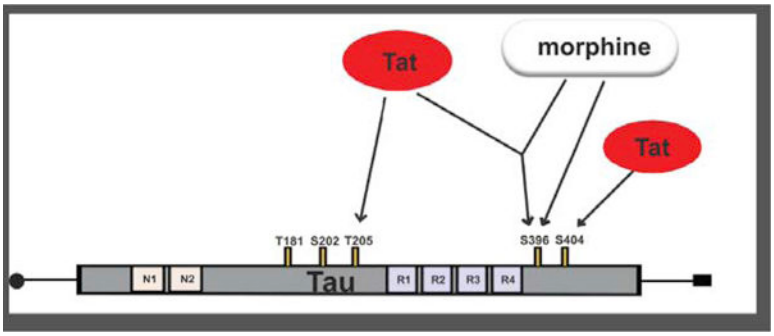

Keywords

Tauopathy; neurofibrillary tangles; sex differences; CDK5/p35; paired helical filament-1; opioid drug abuse

1.0 Introduction

Combined-antiretroviral therapy (cART) has greatly improved the life expectancy of people living with human immunodeficiency virus (HIV) [1]. However, disorders of the central nervous system (CNS) persist even in patients who have attained negligible serum viral titers [2–7]. HIV does not infect neurons but CNS cells like microglia and perivascular macrophages can get infected and serve as viral reservoirs harboring replication-competent viruses and proviruses [8,9]. The presence of a persistent CNS viral reservoir and the longer lifespan of cART-treated HIV-infected individuals raises the question of whether seronegative HIV-infected individuals are predisposed to accelerated brain aging. This possibility has been assessed by examining the CNS deposition of histopathological correlates of Alzheimer's disease (AD) such as neurofibrillary tangles (NFT) and amyloid-β plaques in HIV-infected brains [10–16]. Despite some conflicting reports, a general observation is that the presence of NFT or its precursors in HIV-infected brains is associated with poor neurocognitive outcomes [12,14,17,18]. The current study evaluated the effects of trans-activator of transcription (Tat), a neurotoxic HIV-1 protein, on the distribution of NFT precursors in selected vulnerable brain regions.

NFTs are insoluble aggregates of the detached microtubule-associated protein tau [19–23]. In healthy neurons, neurotransmitters and cargo are transported along microtubules throughout the cell [24]. Tau plays a critical role in maintaining the structural integrity of

microtubules [25,26]. Several phosphorylation sites have been identified on the tau protein. However, phosphorylation at certain serine (Ser) or threonine (Thr) moieties (*e.g.*, Ser 396, 404, 202, 181, Thr 205) mediate pathological tau aggregation or NFT formation [23,27–30]. Phosphorylation at serine 396/404 (pSer396/404), in particular, is thought to decrease the affinity of tau to bind to microtubules [23] thereby initiating a cascade of events leading to NFT formation [27,28]. The two most utilized antibodies for identifying NFT are the paired helical filament-1 (PHF-1) antibody which recognizes tau epitopes phosphorylated at Ser396 and/or Ser404 [31], and the AT8 antibody, which recognizes tau epitopes phosphorylated at Ser202 and/or Thr205 [32]. Increases in PHF-1 and AT8 immunoreactivity have been reported in HIV-infected brains and cerebral spinal fluid (CSF) [11,12,18]. However, the ability to differentiate specific phosphorylated moieties is hampered by the non-specific nature of the PHF-1 and AT8 antibodies. Thus, it is unknown whether increases in PHF-1 or AT8 in HIV brains/CSF are a result of increased phosphorylation at Ser396, Ser404, Ser202, Thr205, or a combination of both for each respective antibody. An understanding of these differences is critical toward understanding neuroHIV pathogenesis and may facilitate the generation of highly specific therapeutics against the initiation of NFT formation.

Opiates are commonly prescribed for pain management in HIV-infected individuals [33,34]. Opiates have a high abuse potential [35–37] and opiate use in the context of HIV is associated with exaggerated neuropathology (for review see [38,39]). Increases in tau phosphorylation at AT8 pathological phosphorylation sites are seen in striatal, cortical, and hippocampal brain regions with chronic opiate abuse [40,41]. The effects of opiates on PHF-1 phosphorylation sites are understudied, and the consequences of opiates and HIV-1 proteins on tau phosphorylation at specific pathological epitopes and brain regions have not been explored. The current study partially addresses these knowledge gaps.

The current study determined whether co-exposure to morphine and HIV-1 Tat enhances pathological phosphorylation of tau at PHF-1 and AT8 phosphorylation sites in the striatum, hippocampus, and frontal cortex of inducible transgenic mice. Neuropathology in HIV-infected individuals is caused in part by neurotoxic viral proteins, *e.g.*, gp120, Vpr and especially Tat, released from infected or activated glial cells and perivascular macrophages [42–46]. By utilizing phospho-specific antibodies against the Ser396, Ser404, Thr205, Ser202 or Thr181 epitopes of tau, we show that co-exposure to morphine and HIV-1 Tat increased phosphorylation at Ser396, in the striatum. By contrast, Tat alone increased tau phosphorylation at Ser404 and Thr205 in the striatum and Ser396 in the hippocampus while morphine increased tau phosphorylation at Ser396 in the prefrontal cortex (PFC). Phosphorylation at Ser202 and Thr181 were not changed by Tat or morphine in any of the regions evaluated.

2.0 Materials and methods

2.1 Animals

Adult male and female mice (4–8 months) were generated at the Virginia Commonwealth University vivarium. Mice were housed 2–5 per cage in an environmentally controlled vivarium (12 h light/dark cycle; lights off at 6 PM). Transgenic (Tg) mice expressing the HIV-1 Tat (Tat^+) or lacking the *tat* transgene (Tat^-) were used. Tat expression in Tg mice

was preferentially targeted to the nervous system through a GFAP-driven reverse tetracycline transactivator (rtTA or tetracycline-on promoter) that was activated by administration of doxycycline (DOX)-containing chow. Tat induction and expression by DOX-administered transgenic mice were confirmed in a previously reported study [47]. Tat^{-} mice nevertheless expressed the rtTA promoter and served as controls as previously described [47,48]. DOX-containing chow (6 g/kg; Harlan Laboratories, Madison, WI) was freely available to both Tat^{+} and Tat^{-} mice for up to 4 weeks. All procedures conformed to the Guide for Care and Use of Laboratory Animals (National Research Council, Washington DC) and were approved by the Virginia Commonwealth University Institutional Animal Care and Use Committee.

2.2 Morphine treatment

Morphine sulfate (National Institute on Drug Abuse Drug Supply Program, Bethesda, MD) dissolved in sterile physiological saline was administered subcutaneously to male Tg mice at a volume of 10μl/g. To mimic the drug taking behavior of opiate-dependent individuals, an escalating dosing regimen was used to induce tolerance, based on previous studies [49,50]. Morphine was administered via twice daily (b.i.d.) ramping doses every 12 h for 14 days: 10 mg/kg on days 1 and 2, 20 mg/kg on days 3 and 4, 30 mg/kg on days 5 and 6, and 40 mg/kg on days 7 – 14,during the last 2 weeks of Tat induction (Fig. 1). For the immunofluorescence studies Tat was induced by DOX administration for 2 weeks coinciding with the start of morphine administration. For the immunoblotting studies DOX was administered for 4 weeks, and morphine was administered starting after 2 weeks of Tat exposure. An equivalent volume of saline was administered to control Tat^{+} and Tat^{-} mice (Fig. 1). Within 5 h of the last injection of morphine or saline, mice were sacrificed, and brain tissues collected. Previous studies using similar regimens suggest somatic signs of spontaneous morphine withdrawal (i.e., jumping, paw tremors, wet dog shakes, or diarrhea) in morphine tolerant mice are not significantly different from saline treated mice after 8 h of the last morphine dose administered [49,51]. In agreement, mice in the current study did not display somatic signs of morphine withdrawal.

2.3 Immunofluorescence

The striatum is particularly vulnerable to the detrimental effects of HIV-1 [52–54]. Previous studies indicated neurodegenerative changes to medium spiny neurons within the striatum after only 2 weeks of Tat exposure [55–57]. Hence, to determine the presence of incipient or frank pathological tau aggregates in morphine- and/or Tat-exposed CNS, we evaluated striatal NFT at the 2-week Tat exposure timepoint. Briefly, isoflurane (4–5%) anesthetized mice were humanely euthanized by intracardiac perfusion with 4% paraformaldehyde in neutral pH phosphate-buffered saline (PBS). Whole brains from Tat^{+} and Tat^{-} male mice administered DOX and morphine/saline for 2 weeks were rapidly removed and post-fixed in fresh paraformaldehyde overnight at 4 °C. Brains were then washed in PBS, incubated in 10% and 20% sucrose, washed again, embedded in Tissue-Tek O.C.T. compound (Sakura Finetek, Torrance, CA), then stored at −80 °C until use. Frozen O.C.T embedded whole brains were sectioned (20 μm-thick) in the coronal plane using a Leica CM cryostat (Leica Biosystems, Buffalo Grove, IL). Tissue sections were permeabilized in a solution containing 0.5% Triton X-100 in phosphate-buffered saline (PBS) for 10 min. Sections were then blocked for 1 h in a solution containing 5% v/v normal serum and 1% w/v bovine serum

albumin in PBS. Following blocking, sections were incubated in mouse monoclonal PHF-1 primary antibody (courtesy of Dr. A. Rory McQuiston; 1:400) and rabbit polyclonal antibody to the neuron-specific antigen NeuN (#ab104225, Abcam, Cambridge, MA; 1:500) overnight at 4 °C. The next day, tissue sections were washed (3 × 10 min) and co-incubated in Alexa Fluor 594 (donkey-anti-rabbit, Invitrogen, Carlsbad, CA; 1:500) and Alexa Fluor 647 (donkey-anti-mouse, Invitrogen, 1:500) secondary antibodies for 1 h at room temperature. Sections were washed (3 × 10 min) following incubation in secondary antibodies and counterstained with Hoechst 33342 (Invitrogen; 1:20,000) to identify nuclei. Photomicrographs of PHF-1-immunoreactive tissues (20×) were taken from bregma +1.32 mm to bregma +0.74 mm using a Zeiss LSM 700 confocal microscope configured to a Zen 2010 software (Zeiss Inc., Thornwood, NY). Images were converted to 8bit grayscale in image J (NIH, Bethesda, MD). To determine the intensity of PHF-1 immunoreactivity, images from two sections (2 images from the dorsolateral striatum per section) were used per mouse. A 4.00 mm^2 field was measured in each tissue section. Background measurements were taken from the corpus callosum (0.64 mm^2 field) of each section and subtracted from the optical density value of the region of interest to generate the corrected pixel intensity values. The corrected pixel intensity values were averaged across the two sections of each mouse. To determine neuron-specific expression of PHF-1 in each tissue section, cells positive for NeuN and PHF-1 were counted manually by a genotype- and treatment-blinded observer with the aid of the ITCN cell-counting plugin for the Image J software. At least, 100 NeuN+ cells from the dorsolateral striatum were counted per section and averaged across two sections for each mouse.

2.4 Immunoblotting

Since Tat and morphine increased striatal PHF-1 immunoreactivity, we next performed immunoblotting to investigate levels of specific pathological phospho-tau epitopes. Tau pathology in Alzheimer's disease is region specific [58], therefore multiple brain regions (i.e., striatum, PFC and hippocampus) were examined. A 4 week timeline of Tat exposure was used based on when PFC and hippocampal associated cognitive deficits are detected in the Tat Tg mouse model used in the current study [55,59–65]. Male mice administered DOX for 4 weeks and morphine for the last 2 weeks of Tat exposure were humanely euthanized by rapid cervical dislocation. A cohort of female mice that were exposed to Tat for 4 weeks were also humanely euthanized to investigate sex-differences in a sub-set of phospho-tau epitopes that were altered by Tat exposure in the striatum of male mice. Whole brains were grossly dissected, flash-frozen in liquid nitrogen, and stored at −80 °C until use. Immunoblotting followed previously published protocols [66–68] with minor modifications. Briefly, fast-frozen striatal, hippocampal, and prefrontal cortical tissues were homogenized in ice-cold RIPA buffer with 1× HALT protease and phosphatase inhibitor cocktail (Thermo Fisher, Waltham, MA). The homogenate was centrifuged at 14,000 rpm for 15 min and the supernatant was aliquoted and stored at −80 °C. Protein concentration was determined using the bicinchoninic acid protein assay method. For immunoblotting, 30 μg of the respective brain samples were electrophoresed on 4–20% Criterion gels and transferred to PVDF membranes. Non-specific binding sites on membranes were blocked overnight with 5% bovine serum albumin in tris buffered saline. Membranes were then incubated overnight in primary antibodies directed against tau (#46687; 1:2,000), pSer202 (#39357; 1:1000),

pThr205 (#49561; 1:1000), pThr181 (#12885; 1:1000), pSer404 (#35834; 1:1000), and pSer396 (#9632; 1:1,000), followed by species-specific secondary antibodies. All antibodies were purchased from Cell Signaling Technology, Danvers, MA. GAPDH (# ab8245, Abcam, Cambridge, MA; 1:2000) was used to assess loading. Membranes were scanned with a ChemiDoc Imager (Bio-Rad, Hercules, CA) and optical density was determined using Image Lab software (V6.0.1, Bio-Rad).

2.5 Sample size determination

For the immunofluorescence assay, our preliminary data suggest that a sample size of 6 in each group has 90% power to detect a difference between means of 70% with a significance level of 0.05. For the immunoblotting assays, preliminary and published data [66] suggest that a sample size of 4 in each group has 90% power to detect a difference between means of 50% with a significance level of 0.05. We, therefore, maintained an n = 6–8/group for all experiments.

2.6 Data analyses

All immunoblotting data were standardized as a percentage (%) of control values (*i.e.*, Tat^{-} mice that received saline). PHF-1 immunofluorescent data were represented as the number of PHF-1+ cells per 100 NeuN+ cells. The data generated were analyzed using a two-way ANOVA followed by a *post hoc* Tukey's multiple comparison test. Pearson's correlation was used to determine the relationship between phosphorylated tau isotypes and tau kinase levels. All analyses were performed using GraphPad Prism software v 8.2 (La Jolla, CA) with significance set at $p < 0.05$. Data are presented as the mean + SEM.

3.0 Results

3.1 Presence of pathological tau aggregates in the striatum of morphine-treated, inducible Tat-transgenic mice.

Striatal PHF-1 was evaluated to determine the presence of pathological tau aggregates in the brains of Tat- and morphine-exposed mice. Evaluation of PHF-1-pixel intensity (Fig. 2C), revealed significant Tat ($F_{1,20} = 20.95$, $p < 0.001$) and morphine ($F_{1,20} = 5.677$, $p = 0.027$) main effects but no interaction ($F_{1,20} = 1.21$, $p = 0.28$). *Post hoc* analysis of relevant planned comparisons revealed significant differences between morphine-treated Tat^{+} (morphine Tat^{+}) mice *vs* morphine Tat^{-} mice and between morphine Tat^{+} mice *vs* saline-treated Tat^{-} (saline Tat^{-}) mice ($p < 0.05$). Evaluation of neuron-specific PHF-1 expression (Fig. 2D), revealed significant Tat ($F_{1,20} = 18.22$, $p < 0.001$) and morphine ($F_{1,20} = 6.05$, $p = 0.02$) main effects but no interaction ($F_{1,20} = 0.80$, $p = 0.38$). *Post hoc* analysis of relevant planned comparisons revealed significant differences between morphine-treated Tat^{+} (morphine Tat^{+}) mice *vs* morphine Tat^{-} mice and between morphine Tat^{+} mice *vs* saline-treated Tat^{-} (saline Tat^{-}) mice ($p < 0.05$).

3.2 Region-specific elevation of phospho-tau isotypes in brains of morphine-treated, inducible Tat-transgenic mice.

To investigate the region-specific effects of chronic exposure to Tat and/or morphine on tau phosphorylation, levels of five pathological phospho-tau isotypes were evaluated in the striatum, hippocampus, and prefrontal cortex.

Analysis of the striatum (Fig. 3A and B), showed significant Tat ($F_{1,24} = 2.13$, $p = 0.0001$) and morphine ($F_{1,24} = 6.68$, $p = 0.02$) main effects, and a significant interaction ($F_{1,24} = 4.33$, $p = 0.04$) for pSer396. Significant Tat main effects were also observed for pSer404 ($F_{1,23} = 4.90$, $p = 0.03$) and pThr205 ($F_{1,20} = 39.30$, $p < 0.0001$) with no significant morphine main effects or interactions (pSer404: $F_{1,23} = 0.38$, $p = 0.54$; $F_{1,23} = 0.03$, $p = 0.87$. pThr205: $F_{1,20} = 1.76$, $p = 0.20$; $F_{1,23} = 2.29$, $p = 0.15$ respectively). In contrast, no significant main effects or interaction were observed for pSer202 ($F_{1,23} = 0.001$, $p = 0.97$; $F_{1,23} = 0.16$, $p = 0.69$; $F_{1,23} = 2.13$, $p = 0.17$ respectively) and pThr181 ($F_{1,21} = 0.81$, $p = 0.38$; $F_{1,21} = 0.16$, $p = 0.70$; $F_{1,21} = 0.18$, $p = 0.67$ respectively). *Post hoc* analysis of relevant planned comparisons revealed significant differences between morphine Tat^+ mice *vs* saline Tat^+ mice, between morphine Tat^+ *vs* morphine Tat^- mice, and between morphine Tat^+ *vs* saline Tat^- mice for pSer396 ($p < 0.05$). Total tau levels were unchanged in any of the groups or brain regions evaluated (data not shown).

Analysis of the hippocampus (Fig. 3C and D), revealed a significant Tat main effect for pSer396 ($F_{1,20} = 7.43$, $p = 0.01$) but no morphine main effect or interaction ($F_{1,20} = 0.35$, $p = 0.55$; $F_{1,20} = 0.05$, $p = 0.83$ respectively). In contrast, pSer404, pThr205, and pThr181 were unchanged in any of the groups evaluated (pSer404: Tat effect, $F_{1,20} = 0.36$, $p = 0.56$; morphine effect, $F_{1,20} = 0.88$, $p = 0.36$; interaction $F_{1,20} = 1.13$, $p = 0.30$. pThr205: $F_{1,20} = 0.03$, $p = 0.87$; $F_{1,20} = 0.42$, $p = 0.52$; $F_{1,20} = 1.93$, $p = 0.18$ respectively. pThr181: $F_{1,20} = 0.76$, $p = 0.40$; $F_{1,20} = 0.79$, $p = 0.38$; $F_{1,20} = 3.52$, $p = 0.08$ respectively). pSer202 was not detected in the hippocampus. No significant differences were observed for any of the planned comparisons.

Analysis of the prefrontal cortex (Fig. 3E and F), showed a significant morphine main effect for pSer396 ($F_{1,20} = 6.52$, $p = 0.02$) but no significant Tat main effect or interaction ($F_{1,20} = 1.79$, $p = 0.2$; $F_{1,20} = 1.99$, $p = 0.17$ respectively). No other main effects or interactions were observed for any of the evaluated phospho-tau isotypes (pSer404: Tat effect, $F_{1,20} = 0.61$, $p = 0.44$; morphine effect, $F_{1,20} = 1.23$, $p = 0.28$; interaction, $F_{1,20} = 0.02$, $p = 0.90$. pThr205: $F_{1,22} = 0.27$, $p = 0.61$; $F_{1,22} = 0.36$, $p = 0.56$; $F_{1,22} = 0.84$, $p = 0.37$ respectively. pSer202: $F_{1,20} = 0.61$, $p = 0.44$; $F_{1,20} = 1.23$, $p = 0.28$; $F_{1,20} = 0.02$, $p = 0.90$ respectively. pThr181: $F_{1,20} = 0.01$, $p = 0.93$; $F_{1,20} = 0.52$, $p = 0.48$; $F_{1,20} = 3.24$, $p = 0.09$ respectively). *Post hoc* analyses of relevant planned comparisons revealed significant differences between morphine Tat^- *vs* saline Tat^- ($p < 0.05$) for pSer396.

3.3 Sex-differences and Tat effects on phospho-tau isotypes

To determine the effect of sex on Tat-induced changes to tau phosphorylation, we compared levels of 3 striatal phospho-tau isotypes (p-tau epitopes in which changes were evident in the striatum of male mice, *i.e.*, p396, p404 and pThr205) between male and female inducible Tat

transgenic mice. There were no significant differences between male and female mice for striatal levels of total tau, pSer396, and pSer404 (Tat effect, $F_{1,21} = 1.60$, $p = 0.70$; sex effect, $F_{1,21} = 0.07$, $p = 0.79$; interaction, $F_{1,21} = 0.11$, $p = 0.74$. pSer396: $F_{1,21} = 0.94$, $p = 0.34$; $F_{1,21} = 2.29$, $p = 0.14$; $F_{1,21} = 1.05$, $p = 0.32$, respectively. pSer404: $F_{1,22} = 0.15$, $p = 0.70$; $F_{1,22} = 3.48$, $p = 0.08$; $F_{1,22} = 3.43$, $p = 0.08$ respectively) (Fig. 4). Striatal pThr205 levels showed significant main effects for Tat ($F_{1,20} = 0.60$, $p = 0.02$), sex ($F_{1,20} = 16.0$, $p = 0.0007$), and interaction ($F_{1,20} = 16.14$, $p = 0.0007$) (Fig. 4). *Post hoc* analyses showed significant differences between male Tat^+ mice *vs* male Tat^- mice, between male Tat^+ mice *vs* female mice irrespective of genotype.

3.4 Differential alterations to tau kinases in the striatum of morphine-treated inducible Tat transgenic mice.

The finding that tau was hyperphosphorylated at Ser396 by Tat ± morphine in the striatum led us to investigate whether two of the tau kinases (GSK3β and CDK5/p35) implicated in the pathological phosphorylation of tau [54] might also be upregulated. There were no significant main effects or interaction for pGSK3β/GSK3β (Tat effect, $F_{1,24} = 1.16$, $p = 0.29$; morphine effects, $F_{1,24} = 0.0001$, $p = 0.99$; interaction, $F_{1,24} = 1.13$, $p = 0.30$) (Fig. 5A and B).

P35 levels showed significant Tat ($F_{1,26} = 14.95$, $p = 0.0007$) and morphine ($F_{1,26} = 11.8$, $p = 0.002$) main effects but no interaction ($F_{1,26} = 0.1$, $p = 0.75$) (Fig. 5A and B). A significant effect of Tat ($F_{1,20} = 6.08$, $p = 0.02$) was also observed for phospho-CDK5 with no morphine effect or interaction ($F_{1,20} = 1.09$, $p = 0.30$; $F_{1,20} = 0.37$, $p = 0.55$ respectively) (Fig. 4A and B). No changes in total CDK5 levels were observed (Tat effect, $F_{1,26} = 1.06$, $p = 0.31$; morphine effect, $F_{1,26} = 0.01$, $p = 0.91$; interaction, $F_{1,26} = 0.01$, $p = 0.93$) (Fig. 5A and B). *Post hoc* analysis revealed significant differences between morphine Tat^+ *vs* saline Tat^+, between morphine Tat^+ *vs* morphine Tat^-, and between morphine Tat^+ *vs* saline Tat^- mice for p35 levels ($p < 0.05$). No other significant *post hoc* comparisons were observed for the other proteins. P35 levels positively correlated with pSer396 levels in morphine Tat^+ mice ($r = 0.75$, $p = 0.02$) (Fig. 5C).

4.0 Discussion

The current study evaluated five pathological phospho-tau isotypes in three brain regions of morphine-treated Tat^+ and Tat^- mice. A significant and specific interaction of morphine and Tat to enhance phosphorylation of tau at Ser396 was found to occur in the striatum, but not in the other regions. There were no interactive effects on Ser404, Thr205, Thr181 or Ser202. Tat by itself increased phosphorylation of tau at Ser404 and Thr205 in the striatum, and at Ser404 in the hippocampus (Fig. 5D). Morphine by itself increased the phosphorylation of tau at Ser396 in the prefrontal cortex (Fig. 5D). Considering prior findings that Tat dysregulates the alternative splicing of *MAPT* exon 10 resulting in the aberrant upregulation of tau isoforms with three microtubule binding domain repeats (3R) [69], our current findings suggest Tat affects tau expression and hyperphosphorylation through multiple, region-specific mechanisms of action that can be selectively altered by co-exposure to morphine.

To investigate whether co-exposure to morphine and Tat increased predisposition to the development of pathological brain hallmarks indicative of accelerated brain aging, levels of pathological phospho-tau isotypes were evaluated in an *in vivo* model of the comorbidity. Few studies have evaluated the effects of HIV-1 Tat on tau phosphorylation. Tau phosphorylation was increased at AT8 phosphorylation sites in human neuroblastoma cells following 48 h of HIV-1 Tat exposure *in vitro* [70], and at PHF-1 site in the hippocampus of Tat transgenic mice [71]. The use of specific antibodies for Thr205, Ser202, Ser396, and Ser404 revealed the specific AT8 and PHF-1 tau phosphorylation sites affected by exposure to HIV-1 Tat. The current study further revealed hyperphosphorylation at Thr205 in male, but not in female, Tat mice. Neuroprotective effects of estrogen [72–74] may explain the disparate outcomes between male and female mice for Thr205. Co-exposure to Tat and the preferential μ-opioid receptor agonist morphine resulted in an interactive increase in the pathological Ser396 phospho-tau moiety suggesting pSer396 as a particularly relevant therapeutic target against tauopathy and NFT aggregation in HIV-infected brains in the context of a comorbid opioid use disorder (Fig. 5D). Phosphorylation of tau at the Ser396 moiety is an important step in the initiation of NFT formation [23,27,28]. Hyperphosphorylation at other pathological sites such as the AT8 region is more evident at the later stages of NFT formation [27]. Hyperphosphorylation of tau at Ser396 without concomitant hyperphosphorylation at Ser202 is thus suggestive of an early stage tau pathology. Increased striatal pSer396 was only observed in brains exposed to both Tat and morphine, but not in age-matched mice from the individual treatment groups. This suggests that co-exposure may predispose to an accelerated deposition of fibrillary tangles/pre-tangles indicative of brain aging.

Tau aggregates are present during normal aging and are predominantly confined to hippocampal and some cortical brain regions [75]. Pathological tau aggregation may occur at relatively earlier ages and increases progressively from subcortical to cortical brain regions with the latter occurring at later stages of Alzheimer's disease [76]. Region-specific effects of Tat ± morphine on tau phosphorylation overlap markedly with previous reports of neurodegenerative changes in the striatum, hippocampus, and prefrontal cortex [55,56,77]. Microtubule depolymerization resulting from tau detachment alters neuronal spine formation [78,79]. The more dramatic pathological changes in striatal tau compared to other brain regions shown in this study may contribute to the relatively high incidence of synaptodendritic injury previously reported in striatal medium spiny neurons [77]. In addition to synaptodendritic injury, tauopathies trigger a variety of pathophysiological processes including the production of amyloid-β (Aβ) plaques in Alzheimer's disease [80,81]. Aggregation of Aβ and hyperphosphorylated tau, particularly in the striatum, is a strong indicator of poor neurocognitive outcomes in familial Alzheimer's disease [82]. Interestingly, Tat can aggregate with, and enhance the deposition of Aβ aggregates [83,84]. Thus, the specific tauopathy observed in the current study may contribute to the pathogenesis of neuroHIV in infected individuals co-exposed to opioids.

Several kinases have been implicated in the pathological phosphorylation of tau, most notably, GSK3β and CDK5/p35 [85]. While GSK3β activation was not observed in the current study, p35, the primary neuronal activator of CDK5 [86] was increased, as were phospho-CDK5 levels. The level of p35 correlated positively with striatal pSer396 amounts

suggesting that CDK5/p35 may be driving tau hyperphosphorylation at Ser396. In neuropathologies in which CDK5 is aberrantly activated, the cleavage of p35 to p25 by calpain is reported to increase the catalytic activity of CDK5 at AT8 tau phosphorylation sites by about 2.4-fold [87]. By contrast, a separate and relatively recent study evaluating the kinetics of CDK5/p35 *vs* CDK5/p25, reported no differences in catalytic activity between the two kinases in phosphorylating tau at pathologic sites [88]. Thus, it is likely that the CDK5/p35 complex initiates aberrant phosphorylation of tau while p25 activation occurs later during the disease process and perpetuates the maladaptive phosphorylation of multiple pathologic sites such as the Ser202 and Thr181 epitopes. This would explain the absence of p25 and tau hyperphosphorylation at Ser202 and Thr181 in the current study. While further testing is required to evaluate these possibilities, observations from the tau kinase studies support the argument that HIV-1 Tat and morphine co-exposure triggers an early-state tauopathy that may progress to additional tau phosphorylation sites with more prolonged exposure.

In conclusion, the current study identifies the Ser396 moiety on tau to be a convergent pathogenic site for HIV-1 Tat and morphine comorbidity in the striatum. This interactive, regional effect may signal the onset of a combined HIV- and morphine-induced pathology analogous to accelerated brain aging. From a therapeutic standpoint, the finding also suggests a specific target for intervention during early stages of tauopathy in such individuals. Longer Tat (*e.g.*, [89]) and/or morphine exposure durations might reveal additional, vulnerable brain regions and/or therapeutic targets.

Acknowledgements

The authors thank Dr. A Rory McQuiston for supplying the paired helical filament-1 antibody for this study. The authors acknowledge funding from the National Institute on Drug Abuse grants R01 DA018633, R01 DA045588, and R01 DA044939, and thank the NIDA Drug Supply Program for assistance.

Abbreviations

cART	Combination antiretroviral therapy
CDK5	Cyclin dependent kinase 5
CNS	Central nervous system
CSF	Cerebrospinal fluid
GSK3β	Glycogen synthase kinase 3 beta
HIV	Human immunodeficiency virus
NFT	Neurofibrillary tangles
PHF-1	Paired helical filament-1
Ser	Serine
Tat	Trans-activator of transcription

Thr	Threonine

References

[1]. Teeraananchai S, Kerr SJ, Amin J, Ruxrungtham K, Law MG, Life expectancy of HIV-positive people after starting combination antiretroviral therapy: a meta-analysis., HIV Med. 18 (2017) 256–266. doi:10.1111/hiv.12421. [PubMed: 27578404]

[2]. Heaton RK, Clifford DB, Franklin DR, Woods SP, Ake C, Vaida F, et al., HIV-associated neurocognitive disorders persist in the era of potent antiretroviral therapy: CHARTER Study., Neurology. 75 (2010) 2087–2096. doi:10.1212/WNL.0b013e318200d727. [PubMed: 21135382]

[3]. Bloch M, Kamminga J, Jayewardene A, Bailey M, Carberry A, Vincent T, et al., A Screening Strategy for HIV-Associated Neurocognitive Disorders That Accurately Identifies Patients Requiring Neurological Review., Clin. Infect. Dis 63 (2016) 687–693. doi:10.1093/cid/ciw399. [PubMed: 27325690]

[4]. De Francesco D, Underwood J, Post FA, Vera JH, Williams I, Boffito M, et al., Defining cognitive impairment in people-living-with-HIV: the POPPY study., BMC Infect. Dis 16 (2016) 617. doi:10.1186/s12879-016-1970-8. [PubMed: 27793128]

[5]. Wright EJ, Grund B, Cysique LA, Robertson KR, Brew BJ, Collins G, et al., Factors associated with neurocognitive test performance at baseline: a substudy of the INSIGHT Strategic Timing of AntiRetroviral Treatment (START) trial., HIV Med. 16 Suppl 1 (2015) 97–108. doi:10.1111/hiv.12238. [PubMed: 25711328]

[6]. Crum-Cianflone NF, Moore DJ, Letendre S, Poehlman Roediger M, Eberly L, Weintrob A, et al., Low prevalence of neurocognitive impairment in early diagnosed and managed HIV-infected persons., Neurology. 80 (2013) 371–379. doi:10.1212/WNL.0b013e31827f0776. [PubMed: 23303852]

[7]. Rahimy E, Li F-Y, Hagberg L, Fuchs D, Robertson K, Meyerhoff DJ, et al., Blood-Brain Barrier Disruption Is Initiated During Primary HIV Infection and Not Rapidly Altered by Antiretroviral Therapy., J. Infect. Dis 215 (2017) 1132–1140. doi:10.1093/infdis/jix013. [PubMed: 28368497]

[8]. Saksena NK, Wang B, Zhou L, Soedjono M, Ho YS, Conceicao V, HIV reservoirs in vivo and new strategies for possible eradication of HIV from the reservoir sites., HIV AIDS (Auckl). 2 (2010) 103–122. [PubMed: 22096389]

[9]. Joseph SB, Kincer LP, Bowman NM, Evans C, Vinikoor MJ, Lippincott CK, et al., Human Immunodeficiency Virus Type 1 RNA Detected in the Central Nervous System (CNS) After Years of Suppressive Antiretroviral Therapy Can Originate from a Replicating CNS Reservoir or Clonally Expanded Cells., Clin. Infect. Dis 69 (2019) 1345–1352. doi:10.1093/cid/ciy1066. [PubMed: 30561541]

[10]. Gisslén M, Krut J, Andreasson U, Blennow K, Cinque P, Brew BJ, et al., Amyloid and tau cerebrospinal fluid biomarkers in HIV infection., BMC Neurol. 9 (2009) 63. doi:10.1186/1471-2377-9-63. [PubMed: 20028512]

[11]. Anthony IC, Ramage SN, Carnie FW, Simmonds P, Bell JE, Accelerated Tau deposition in the brains of individuals infected with human immunodeficiency virus-1 before and after the advent of highly active anti-retroviral therapy., Acta Neuropathol. 111 (2006) 529–538. doi:10.1007/s00401-006-0037-0. [PubMed: 16718349]

[12]. Patrick C, Crews L, Desplats P, Dumaop W, Rockenstein E, Achim CL, et al., Increased CDK5 expression in HIV encephalitis contributes to neurodegeneration via tau phosphorylation and is reversed with Roscovitine., Am. J. Pathol 178 (2011) 1646–1661. doi:10.1016/j.ajpath.2010.12.033. [PubMed: 21435449]

[13]. Smith DB, Simmonds P, Bell JE, Brain viral burden, neuroinflammation and neurodegeneration in HAART-treated HIV positive injecting drug users., J. Neurovirol 20 (2014) 28–38. doi:10.1007/s13365-013-0225-3. [PubMed: 24420447]

[14]. Steinbrink F, Evers S, Buerke B, Young P, Arendt G, Koutsilieri E, et al., Cognitive impairment in HIV infection is associated with MRI and CSF pattern of neurodegeneration., Eur. J. Neurol 20 (2013) 420–428. doi:10.1111/ene.12006. [PubMed: 23095123]

[15]. Mohamed M, Skolasky RL, Zhou Y, Ye W, Brasic JR, Brown A, et al., Beta-amyloid (Aβ) uptake by PET imaging in older HIV+ and HIV− individuals., J. Neurovirol (2020). doi:10.1007/s13365-020-00836-1.

[16]. Fields JA, Swinton MK, Soontornniyomkij B, Carson A, Achim CL, Beta amyloid levels in CSF of HIV-infected people vary by exposure to antiretroviral therapy., AIDS. (2020). doi:10.1097/QAD.0000000000002506.

[17]. Green AJ, Giovannoni G, Hall-Craggs MA, Thompson EJ, Miller RF, Cerebrospinal fluid tau concentrations in HIV infected patients with suspected neurological disease., Sex. Transm. Infect 76 (2000) 443–446. doi:10.1136/sti.76.6.443. [PubMed: 11221126]

[18]. Brew BJ, Pemberton L, Blennow K, Wallin A, Hagberg L, CSF amyloid beta42 and tau levels correlate with AIDS dementia complex., Neurology. 65 (2005) 1490–1492. doi:10.1212/01.wnl.0000183293.95787.b7. [PubMed: 16275845]

[19]. Delacourte A, Défossez A, [Biochemical characterization of an immune serum which specifically marks neurons in neurofibrillary degeneration in Alzheimer's disease]., C R Acad Sci III, Sci Vie. 303 (1986) 439–444.

[20]. Lee VM, Otvos L, Carden MJ, Hollosi M, Dietzschold B, Lazzarini RA, Identification of the major multiphosphorylation site in mammalian neurofilaments., Proc. Natl. Acad. Sci. USA 85 (1988) 1998–2002. doi:10.1073/pnas.85.6.1998. [PubMed: 2450354]

[21]. Trojanowski JQ, Schmidt ML, Otvos L, Gur RC, Gur RE, Hurtig H, et al., Selective expression of epitopes in multiphosphorylation repeats of the high and middle molecular weight neurofilament proteins in Alzheimer neurofibrillary tangles., Ann. Med 21 (1989) 113–116. doi:10.3109/07853898909149196. [PubMed: 2475147]

[22]. Bancher C, Brunner C, Lassmann H, Budka H, Jellinger K, Wiche G, et al., Accumulation of abnormally phosphorylated tau precedes the formation of neurofibrillary tangles in Alzheimer's disease., Brain Res. 477 (1989) 90–99. doi:10.1016/0006-8993(89)91396-6. [PubMed: 2495152]

[23]. Bramblett GT, Goedert M, Jakes R, Merrick SE, Trojanowski JQ, Lee VM, Abnormal tau phosphorylation at Ser396 in Alzheimer's disease recapitulates development and contributes to reduced microtubule binding., Neuron. 10 (1993) 1089–1099. doi:10.1016/0896-6273(93)90057-x. [PubMed: 8318230]

[24]. Kelliher MT, Saunders HA, Wildonger J, Microtubule control of functional architecture in neurons., Curr. Opin. Neurobiol 57 (2019) 39–45. doi:10.1016/j.conb.2019.01.003. [PubMed: 30738328]

[25]. Caceres A, Kosik KS, Inhibition of neurite polarity by tau antisense oligonucleotides in primary cerebellar neurons., Nature. 343 (1990) 461–463. doi:10.1038/343461a0. [PubMed: 2105469]

[26]. Weingarten MD, Lockwood AH, Hwo SY, Kirschner MW, A protein factor essential for microtubule assembly., Proc. Natl. Acad. Sci. USA 72 (1975) 1858–1862. doi:10.1073/pnas.72.5.1858. [PubMed: 1057175]

[27]. Mondragón-Rodríguez S, Perry G, Luna-Muñoz J, Acevedo-Aquino MC, Williams S, Phosphorylation of tau protein at sites Ser(396–404) is one of the earliest events in Alzheimer's disease and Down syndrome., Neuropathol Appl Neurobiol. 40 (2014) 121–135. doi:10.1111/nan.12084. [PubMed: 24033439]

[28]. Regalado-Reyes M, Furcila D, Hernández F, Ávila J, DeFelipe J, León-Espinosa G, Phospho-Tau Changes in the Human CA1 During Alzheimer's Disease Progression., J. Alzheimers Dis 69 (2019) 277–288. doi:10.3233/JAD-181263. [PubMed: 30958368]

[29]. Lasagna-Reeves CA, Castillo-Carranza DL, Sengupta U, Sarmiento J, Troncoso J, Jackson GR, et al., Identification of oligomers at early stages of tau aggregation in Alzheimer's disease., FASEB J. 26 (2012) 1946–1959. doi:10.1096/fj.11-199851. [PubMed: 22253473]

[30]. Götz J, Gladbach A, Pennanen L, van Eersel J, Schild A, David D, et al., Animal models reveal role for tau phosphorylation in human disease., Biochim. Biophys. Acta 1802 (2010) 860–871. doi:10.1016/j.bbadis.2009.09.008. [PubMed: 19751831]

[31]. Otvos L, Feiner L, Lang E, Szendrei GI, Goedert M, Lee VM, Monoclonal antibody PHF-1 recognizes tau protein phosphorylated at serine residues 396 and 404., J. Neurosci. Res 39 (1994) 669–673. doi:10.1002/jnr.490390607. [PubMed: 7534834]

[32]. Goedert M, Jakes R, Vanmechelen E, Monoclonal antibody AT8 recognises tau protein phosphorylated at both serine 202 and threonine 205., Neurosci. Lett 189 (1995) 167–169. doi:10.1016/0304-3940(95)11484-e. [PubMed: 7624036]

[33]. Lake S, Kerr T, Buxton J, Guillemi S, Parashar S, Montaner J, et al., Prescription Opioid Injection Among HIV-Positive People Who Inject Drugs in a Canadian Setting., AIDS Behav. 20 (2016) 2941–2949. doi:10.1007/s10461-016-1369-y. [PubMed: 27146887]

[34]. Silverberg MJ, Ray GT, Saunders K, Rutter CM, Campbell CI, Merrill JO, et al., Prescription long-term opioid use in HIV-infected patients., Clin. J. Pain 28 (2012) 39–46. doi:10.1097/AJP.0b013e3182201a0f. [PubMed: 21677568]

[35]. Varshney U, Mobile Health Interventions for Opioid Epidemic, (2019). https://aisel.aisnet.org/amcis2019/treo/treos/77/

[36]. Kolodny A, Courtwright DT, Hwang CS, Kreiner P, Eadie JL, Clark TW, et al., The prescription opioid and heroin crisis: a public health approach to an epidemic of addiction., Annu. Rev. Public Health 36 (2015) 559–574. doi:10.1146/annurev-publhealth-031914-122957. [PubMed: 25581144]

[37]. Hser Y-I, Evans E, Grella C, Ling W, Anglin D, Long-term course of opioid addiction., Harv. Rev. Psychiatry 23 (2015) 76–89. doi:10.1097/HRP.0000000000000052. [PubMed: 25747921]

[38]. Murphy A, Barbaro J, Martínez-Aguado P, Chilunda V, Jaureguiberry-Bravo M, Berman JW, The effects of opioids on HIV neuropathogenesis., Front. Immunol 10 (2019) 2445. doi:10.3389/fimmu.2019.02445. [PubMed: 31681322]

[39]. Fitting S, McRae M, Hauser KF, Opioid and neuroHIV Comorbidity - Current and Future Perspectives., J Neuroimmune Pharmacol. (2020). doi:10.1007/s11481-020-09941-8.

[40]. Kovacs GG, Horvath MC, Majtenyi K, Lutz MI, Hurd YL, Keller E, Heroin abuse exaggerates age-related deposition of hyperphosphorylated tau and p62-positive inclusions., Neurobiol. Aging 36 (2015) 3100–3107. doi:10.1016/j.neurobiolaging.2015.07.018. [PubMed: 26254956]

[41]. Anthony IC, Norrby KE, Dingwall T, Carnie FW, Millar T, Arango JC, et al., Predisposition to accelerated Alzheimer-related changes in the brains of human immunodeficiency virus negative opiate abusers., Brain. 133 (2010) 3685–3698. doi:10.1093/brain/awq263. [PubMed: 21126996]

[42]. Ensoli B, Buonaguro L, Barillari G, Fiorelli V, Gendelman R, Morgan RA, et al., Release, uptake, and effects of extracellular human immunodeficiency virus type 1 Tat protein on cell growth and viral transactivation., J. Virol 67 (1993) 277–287. [PubMed: 8416373]

[43]. Tornatore C, Meyers K, Atwood W, Conant K, Major E, Temporal patterns of human immunodeficiency virus type 1 transcripts in human fetal astrocytes., J. Virol 68 (1994) 93–102. [PubMed: 8254781]

[44]. Nath A, Human immunodeficiency virus (HIV) proteins in neuropathogenesis of HIV dementia., J. Infect. Dis 186 Suppl 2 (2002) S193–8. doi:10.1086/344528. [PubMed: 12424697]

[45]. Salemi J, Obregon DF, Cobb A, Reed S, Sadic E, Jin J, et al., Flipping the switches: CD40 and CD45 modulation of microglial activation states in HIV associated dementia (HAD)., Mol. Neurodegener 6 (2011) 3. doi:10.1186/1750-1326-6-3. [PubMed: 21223591]

[46]. Lutgen V, Narasipura SD, Barbian HJ, Richards M, Wallace J, Razmpour R, et al., HIV infects astrocytes in vivo and egresses from the brain to the periphery., PLoS Pathog. 16 (2020) e1008381. doi:10.1371/journal.ppat.1008381. [PubMed: 32525948]

[47]. Bruce-Keller AJ, Turchan-Cholewo J, Smart EJ, Geurin T, Chauhan A, Reid R, et al., Morphine causes rapid increases in glial activation and neuronal injury in the striatum of inducible HIV-1 Tat transgenic mice., Glia. 56 (2008) 1414–1427. doi:10.1002/glia.20708. [PubMed: 18551626]

[48]. Hauser KF, Hahn YK, Adjan VV, Zou S, Buch SK, Nath A, et al., HIV-1 Tat and morphine have interactive effects on oligodendrocyte survival and morphology., Glia. 57 (2009) 194–206. doi:10.1002/glia.20746. [PubMed: 18756534]

[49]. Papaleo F, Contarino A, Gender- and morphine dose-linked expression of spontaneous somatic opiate withdrawal in mice., Behav. Brain Res 170 (2006) 110–118. doi:10.1016/j.bbr.2006.02.009. [PubMed: 16580078]

[50]. Bryant CD, Eitan S, Sinchak K, Fanselow MS, Evans CJ, NMDA receptor antagonism disrupts the development of morphine analgesic tolerance in male, but not female C57BL/6J mice., Am. J.

Physiol. Regul. Integr. Comp. Physiol 291 (2006) R315–26. doi:10.1152/ajpregu.00831.2005. [PubMed: 16601258]

[51]. Papaleo F, Kitchener P, Contarino A, Disruption of the CRF/CRF1 receptor stress system exacerbates the somatic signs of opiate withdrawal., Neuron. 53 (2007) 577–589. doi:10.1016/j.neuron.2007.01.022. [PubMed: 17296558]

[52]. Ellis R, Langford D, Masliah E, HIV and antiretroviral therapy in the brain: neuronal injury and repair., Nat. Rev. Neurosci 8 (2007) 33–44. doi:10.1038/nrn2040. [PubMed: 17180161]

[53]. McArthur JC, Steiner J, Sacktor N, Nath A, Human immunodeficiency virus-associated neurocognitive disorders: Mind the gap., Ann. Neurol 67 (2010) 699–714. doi:10.1002/ana.22053. [PubMed: 20517932]

[54]. Nath A, Eradication of human immunodeficiency virus from brain reservoirs., J. Neurovirol 21 (2015) 227–234. doi:10.1007/s13365-014-0291-1. [PubMed: 25366659]

[55]. Nass SR, Hahn YK, McLane VD, Varshneya NB, Damaj MI, Knapp PE, et al., Chronic HIV-1 Tat exposure alters anterior cingulate cortico-basal ganglia-thalamocortical synaptic circuitry, associated behavioral control, and immune regulation in male mice., Brain Behav. Immun. Health 5 (2020). doi:10.1016/j.bbih.2020.100077.

[56]. Fitting S, Ignatowska-Jankowska BM, Bull C, Skoff RP, Lichtman AH, Wise LE, et al., Synaptic dysfunction in the hippocampus accompanies learning and memory deficits in human immunodeficiency virus type-1 Tat transgenic mice., Biol. Psychiatry 73 (2013) 443–453. doi:10.1016/j.biopsych.2012.09.026. [PubMed: 23218253]

[57]. Schier CJ, Marks WD, Paris JJ, Barbour AJ, McLane VD, Maragos WF, et al., Selective Vulnerability of Striatal D2 versus D1 Dopamine Receptor-Expressing Medium Spiny Neurons in HIV-1 Tat Transgenic Male Mice., J. Neurosci 37 (2017) 5758–5769. doi:10.1523/JNEUROSCI.0622-17.2017. [PubMed: 28473642]

[58]. Hu W, Wu F, Zhang Y, Gong C-X, Iqbal K, Liu F, Expression of Tau Pathology-Related Proteins in Different Brain Regions: A Molecular Basis of Tau Pathogenesis., Front. Aging Neurosci 9 (2017) 311. doi:10.3389/fnagi.2017.00311. [PubMed: 29021756]

[59]. Marks WD, Paris JJ, Schier CJ, Denton MD, Fitting S, McQuiston AR, et al., HIV-1 Tat causes cognitive deficits and selective loss of parvalbumin, somatostatin, and neuronal nitric oxide synthase expressing hippocampal CA1 interneuron subpopulations., J. Neurovirol 22 (2016) 747–762. doi:10.1007/s13365-016-0447-2. [PubMed: 27178324]

[60]. Hahn YK, Paris JJ, Lichtman AH, Hauser KF, Sim-Selley LJ, Selley DE, et al., Central HIV-1 Tat exposure elevates anxiety and fear conditioned responses of male mice concurrent with altered mu-opioid receptor-mediated G-protein activation and β-arrestin 2 activity in the forebrain., Neurobiol. Dis 92 (2016) 124–136. doi:10.1016/j.nbd.2016.01.014. [PubMed: 26845176]

[61]. Paris JJ, Zou S, Hahn YK, Knapp PE, Hauser KF, 5α-reduced progestogens ameliorate mood-related behavioral pathology, neurotoxicity, and microgliosis associated with exposure to HIV-1 Tat., Brain Behav. Immun 55 (2016) 202–214. doi:10.1016/j.bbi.2016.01.007. [PubMed: 26774528]

[62]. Hahn YK, Podhaizer EM, Farris SP, Miles MF, Hauser KF, Knapp PE, Effects of chronic HIV-1 Tat exposure in the CNS: heightened vulnerability of males versus females to changes in cell numbers, synaptic integrity, and behavior., Brain Struct. Funct 220 (2015) 605–623. doi:10.1007/s00429-013-0676-6. [PubMed: 24352707]

[63]. Jacobs IR, Xu C, Hermes DJ, League AF, Xu C, Nath B, et al., Inhibitory Control Deficits Associated with Upregulation of CB1R in the HIV-1 Tat Transgenic Mouse Model of Hand., J Neuroimmune Pharmacol. 14 (2019) 661–678. doi:10.1007/s11481-019-09867-w. [PubMed: 31372820]

[64]. Nookala AR, Schwartz DC, Chaudhari NS, Glazyrin A, Stephens EB, Berman NEJ, et al., Methamphetamine augment HIV-1 Tat mediated memory deficits by altering the expression of synaptic proteins and neurotrophic factors., Brain Behav. Immun 71 (2018) 37–51. doi:10.1016/j.bbi.2018.04.018. [PubMed: 29729322]

[65]. Qrareya AN, Mahdi F, Kaufman MJ, Ashpole NM, Paris JJ, HIV-1 Tat promotes age-related cognitive, anxiety-like, and antinociceptive impairments in female mice that are moderated by aging and endocrine status., Geroscience. (2020). doi:10.1007/s11357-020-00268-z.

[66]. Cho Y-E, Lee M-H, Song B-J, Neuronal Cell Death and Degeneration through Increased Nitroxidative Stress and Tau Phosphorylation in HIV-1 Transgenic Rats., PLoS One. 12 (2017) e0169945. doi:10.1371/journal.pone.0169945. [PubMed: 28107387]

[67]. Ohene-Nyako M, Persons AL, Napier TC, Region-specific changes in markers of neuroplasticity revealed in HIV-1 transgenic rats by low-dose methamphetamine., Brain Struct. Funct 223 (2018) 3503–3513. doi:10.1007/s00429-018-1701-6. [PubMed: 29931627]

[68]. Ohene-Nyako M, Persons AL, Napier TC, Hippocampal blood-brain barrier of methamphetamine self-administering HIV-1 transgenic rats., Eur. J. Neurosci (2020). doi:10.1111/ejn.14925.

[69]. Kadri F, Pacifici M, Wilk A, Parker-Struckhoff A, Del Valle L, Hauser KF, et al., HIV-1-Tat Protein Inhibits SC35-mediated Tau Exon 10 Inclusion through Up-regulation of DYRK1A Kinase., J. Biol. Chem 290 (2015) 30931–30946. doi:10.1074/jbc.M115.675751. [PubMed: 26534959]

[70]. Soliman ML, Geiger JD, Chen X, Caffeine Blocks HIV-1 Tat-Induced Amyloid Beta Production and Tau Phosphorylation., J Neuroimmune Pharmacol. 12 (2017) 163–170. doi:10.1007/s11481-016-9707-4. [PubMed: 27629410]

[71]. Fields JA, Dumaop W, Crews L, Adame A, Spencer B, Metcalf J, et al., Mechanisms of HIV-1 Tat neurotoxicity via CDK5 translocation and hyper-activation: role in HIV-associated neurocognitive disorders., Curr HIV Res. 13 (2015) 43–54. doi:10.2174/1570162×13666150311164201. [PubMed: 25760044]

[72]. Overk CR, Lu P-Y, Wang Y-T, Choi J, Shaw JW, Thatcher GR, et al., Effects of aromatase inhibition versus gonadectomy on hippocampal complex amyloid pathology in triple transgenic mice., Neurobiol. Dis 45 (2012) 479–487. doi:10.1016/j.nbd.2011.08.035. [PubMed: 21945538]

[73]. Rocca WA, Bower JH, Maraganore DM, Ahlskog JE, Grossardt BR, de Andrade M, et al., Increased risk of parkinsonism in women who underwent oophorectomy before menopause., Neurology. 70 (2008) 200–209. doi:10.1212/01.wnl.0000280573.30975.6a. [PubMed: 17761549]

[74]. Kireev RA, Vara E, Viña J, Tresguerres JAF, Melatonin and oestrogen treatments were able to improve neuroinflammation and apoptotic processes in dentate gyrus of old ovariectomized female rats., Age (Omaha). 36 (2014) 9707. doi:10.1007/s11357-014-9707-3.

[75]. Sengoku R, Aging and Alzheimer's disease pathology., Neuropathology. 40 (2020) 22–29. doi:10.1111/neup.12626. [PubMed: 31863504]

[76]. Braak H, Braak E, Neuropathological stageing of Alzheimer-related changes., Acta Neuropathol. 82 (1991) 239–259. doi:10.1007/BF00308809. [PubMed: 1759558]

[77]. Fitting S, Xu R, Bull C, Buch SK, El-Hage N, Nath A, et al., Interactive comorbidity between opioid drug abuse and HIV-1 Tat: chronic exposure augments spine loss and sublethal dendritic pathology in striatal neurons., Am. J. Pathol 177 (2010) 1397–1410. doi:10.2353/ajpath.2010.090945. [PubMed: 20651230]

[78]. Gu J, Firestein BL, Zheng JQ, Microtubules in dendritic spine development., J. Neurosci 28 (2008) 12120–12124. doi:10.1523/JNEUROSCI.2509-08.2008. [PubMed: 19005076]

[79]. Gu J, Zheng JQ, Microtubules in dendritic spine development and plasticity., Open Neurosci. J 3 (2009) 128–133. doi:10.2174/1874082000903020128. [PubMed: 20333314]

[80]. Bloom GS, Amyloid-β and tau: the trigger and bullet in Alzheimer disease pathogenesis., JAMA Neurol. 71 (2014) 505–508. doi:10.1001/jamaneurol.2013.5847. [PubMed: 24493463]

[81]. Kent SA, Spires-Jones TL, Durrant CS, The physiological roles of tau and Aβ: implications for Alzheimer's disease pathology and therapeutics., Acta Neuropathol. 140 (2020) 417–447. doi:10.1007/s00401-020-02196-w. [PubMed: 32728795]

[82]. Hanseeuw BJ, Lopera F, Sperling RA, Norton DJ, Guzman-Velez E, Baena A, et al., Striatal amyloid is associated with tauopathy and memory decline in familial Alzheimer's disease., Alzheimers Res. Ther 11 (2019) 17. doi:10.1186/s13195-019-0468-1. [PubMed: 30717814]

[83]. Hategan A, Masliah E, Nath A, HIV and Alzheimer's disease: complex interactions of HIV-Tat with amyloid β peptide and Tau protein., J. Neurovirol 25 (2019) 648–660. doi:10.1007/s13365-019-00736-z. [PubMed: 31016584]

[84]. Hategan A, Bianchet MA, Steiner J, Karnaukhova E, Masliah E, Fields A, et al., HIV Tat protein and amyloid-β peptide form multifibrillar structures that cause neurotoxicity., Nat. Struct. Mol. Biol 24 (2017) 379–386. doi:10.1038/nsmb.3379. [PubMed: 28218748]

[85]. Martin L, Latypova X, Wilson CM, Magnaudeix A, Perrin M-L, Yardin C, et al., Tau protein kinases: involvement in Alzheimer's disease., Ageing Res Rev. 12 (2013) 289–309. doi:10.1016/j.arr.2012.06.003. [PubMed: 22742992]

[86]. Kanungo J, Zheng Y, Amin ND, Pant HC, Targeting Cdk5 activity in neuronal degeneration and regeneration, Cellular and molecular …. (2009).

[87]. Hashiguchi M, Saito T, Hisanaga S, Hashiguchi T, Truncation of CDK5 activator p35 induces intensive phosphorylation of Ser202/Thr205 of human tau., J. Biol. Chem 277 (2002) 44525–44530. doi:10.1074/jbc.M207426200. [PubMed: 12226093]

[88]. Peterson DW, Ando DM, Taketa DA, Zhou H, Dahlquist FW, Lew J, No difference in kinetics of tau or histone phosphorylation by CDK5/p25 versus CDK5/p35 in vitro., Proc. Natl. Acad. Sci. USA 107 (2010) 2884–2889. doi:10.1073/pnas.0912718107. [PubMed: 20133653]

[89]. Dickens AM, Yoo SW, Chin AC, Xu J, Johnson TP, Trout AL, et al., Chronic low-level expression of HIV-1 Tat promotes a neurodegenerative phenotype with aging., Sci. Rep 7 (2017) 7748. doi:10.1038/s41598-017-07570-5. [PubMed: 28798382]

Highlights

- Co-exposure to HIV-1 Tat and morphine increased striatal tau phosphorylation
- Morphine exposure increased tau phosphorylation in the prefrontal cortex
- HIV-1 Tat exposure increased tau phosphorylation in the hippocampus and striatum
- Interactive tauopathy induced by Tat and morphine resembles accelerated brain aging
- Tat and morphine may selectively phosphorylate specific pathologic tau epitopes

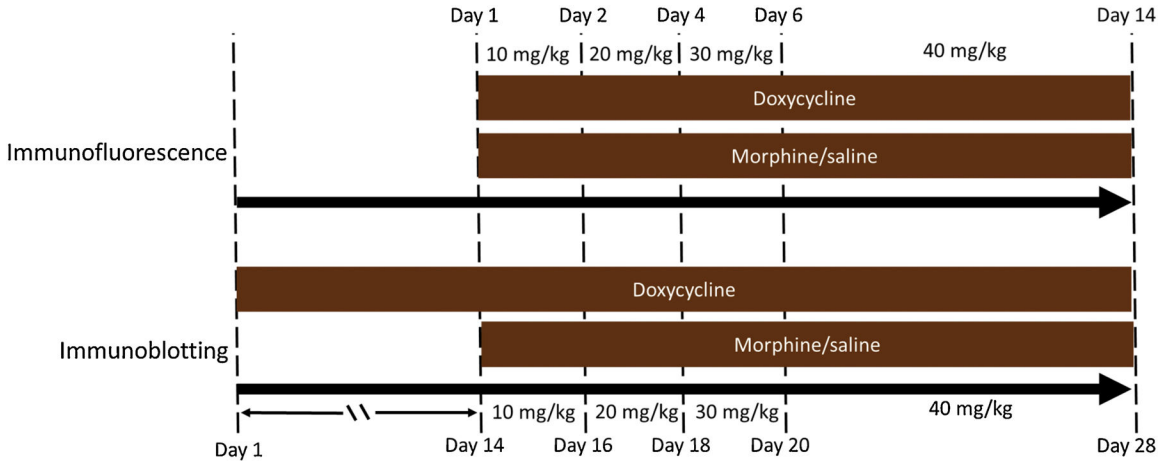

Fig. 1.

Experimental timeline. For 2 weeks, Tat^{+} and Tat^{-} transgenic mice in cohort 1 were administered doxycycline (DOX) supplemented chow to induce Tat expression. Starting on day 1 of DOX administration, cohort 1 mice were repeatedly injected with escalating doses of morphine (10 – 40 mg/kg, s.c., that was increased by 10 mg/kg increments at 2 day intervals) or saline (b.i.d.) for 2 weeks and the brains were harvested for immunohistochemistry. Cohort 2 mice received DOX for 4 weeks. During the final 2 weeks of DOX administration, starting on day 14, mice were additionally injected with the same escalating morphine dosing paradigm as in cohort 1. Mice were humanely euthanized, and the PFC, striatum, and hippocampus were dissected for immunoblotting.

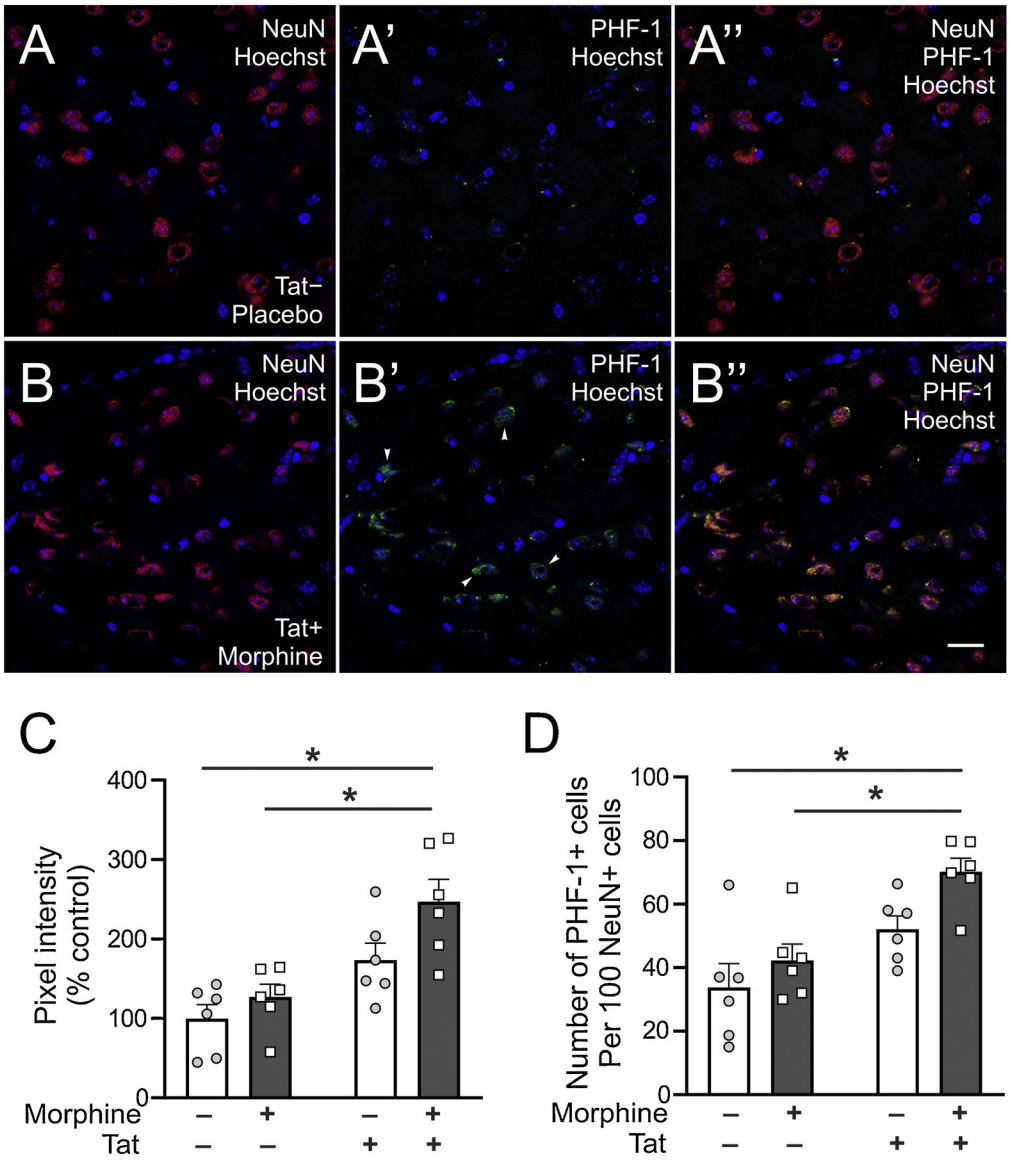

Fig. 2.

Striatal PHF-1 immunoreactivity. (**A and B**) Representative photomicrographs (63×) showing increased PHF-1 immunoreactivity in the striatum of Tat^{-} control mice (**A**) and morphine-treated Tat^{+} (**B**) mice. Scale bar; lower panel = 20 μm. Arrowheads show PHF-1 stained cells. (**C**) Striatal PHF-1 immunoreactivity was increased in mice co-exposed to Tat and morphine compared to Tat^{-} mice irrespective of treatment. (**D**) Neuron-specific expression of PHF-1 was increased in mice co-exposed to Tat and morphine compared to Tat^{-} mice irrespective of treatment. Data are expressed as the mean ± SEM. * indicates planned contrasts that showed differences using Tukey's *post hoc* test ($p < 0.05$). NeuN: neuronal marker, Hoechst: nuclear counterstain, PHF-1: Paired helical filament-1 antibody for detection of tau neurofibrillary tangles phosphorylated at serine 396/404. n = 6/group.

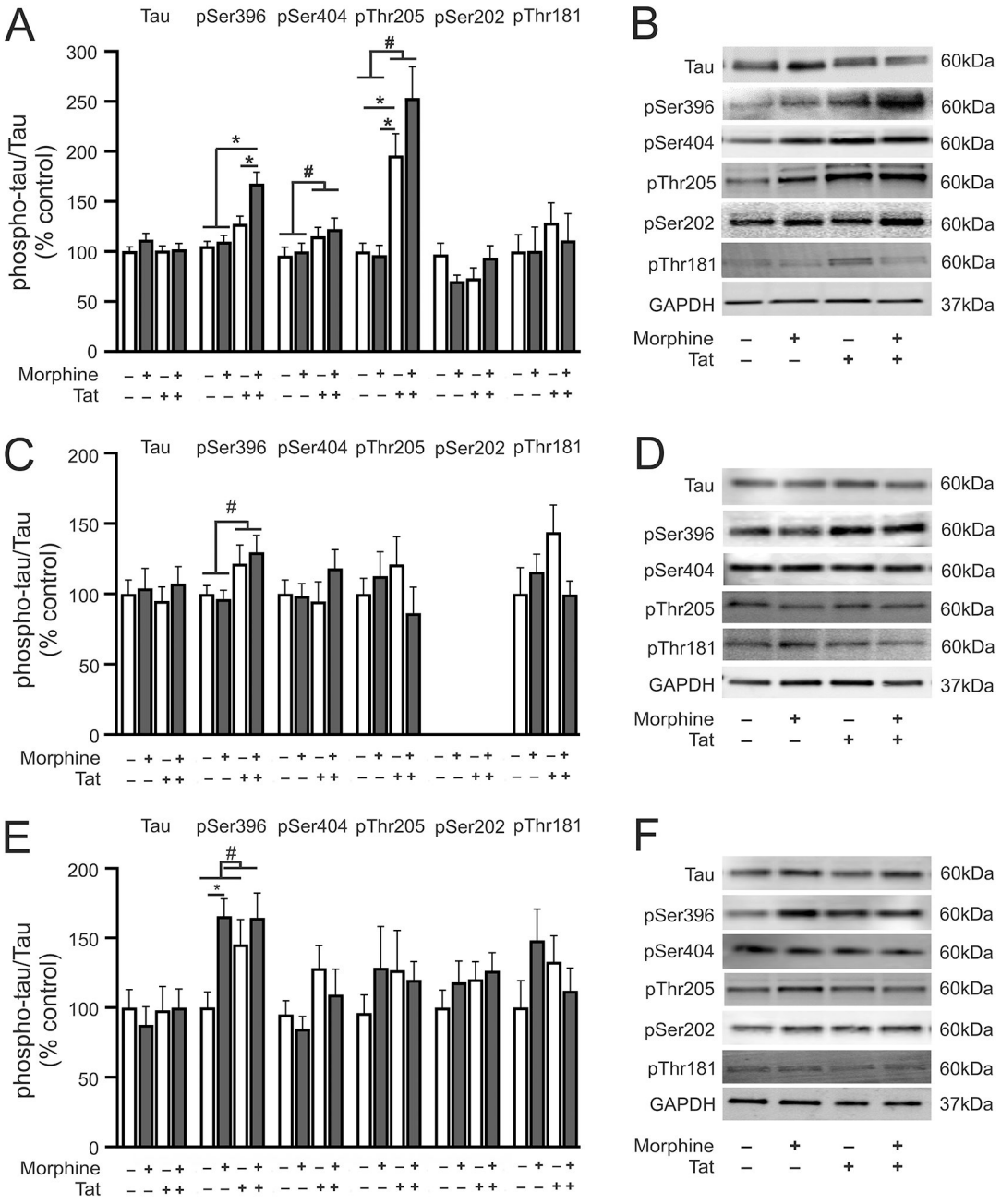

Fig. 3.

Phosphorylated tau protein levels in the striatum, hippocampus, and prefrontal cortex. (**A**) pSer396 level was increased in the striatum of morphine-treated Tat transgenic mice as compared to all other treatment groups. pSer404 and pThr205 levels were increased in the striatum of Tat transgenic mice irrespective of treatment. Striatal pSer202 and pThr181 levels were unchanged in any of the treatment groups evaluated. (**B**) Representative immunoblot images of tau, pSer396, pSer404, pThr205, pSer202, pThr181, and GAPDH in the striatum. (**C**) pSer396 level was increased in the hippocampus of Tat transgenic mice irrespective of treatment. Hippocampal pSer404, pThr205, and pThr181 levels were unchanged in all the treatment groups evaluated. pSer202 level was not detected in the

hippocampus. (**D**) Representative immunoblot images of tau, pSer396, pSer404, pThr205, pThr181, and GAPDH in the hippocampus. (**E**) Morphine treatment increased pSer396 level in the prefrontal cortex of non-Tat transgenic mice. Prefrontal cortex pSer404, pThr205, pSer202, and pThr181, levels were unchanged in all the treatment groups evaluated. (**F**) Representative immunoblot images of tau, pSer396, pSer404, pThr205, pSer202, pThr181, and GAPDH in the prefrontal cortex. Data are expressed as the mean ± SEM. # indicates significant main effects by two-way ANOVA. * indicates planned contrasts that showed differences with Tukey's *post hoc* test ($p < 0.05$). p: phosphorylated tau, Ser: serine. n = 6–8/group.

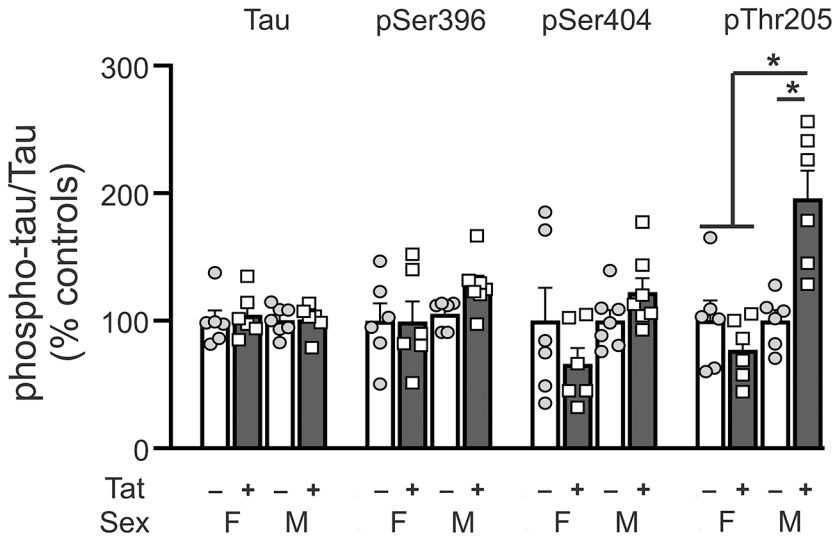

Fig. 4.

Phosphorylated tau protein levels in the striatum of Tat (+/−) female *vs* male mice. No significant differences were observed between Tat (+/−) female and male mice for striatal pSer396 and pSer404 levels. Striatal pThr205 levels were increased in male Tat^{+} mice relative to male Tat^{-} mice and female mice. Data are expressed as mean ± SEM. # indicates significant main effects by two-way ANOVA. * indicates planned contrasts that showed differences with Tukey's *post hoc* test ($p < 0.05$). p: phosphorylated tau, Ser: serine, Thr: threonine, F: female, M: male. n = 6–7/group.

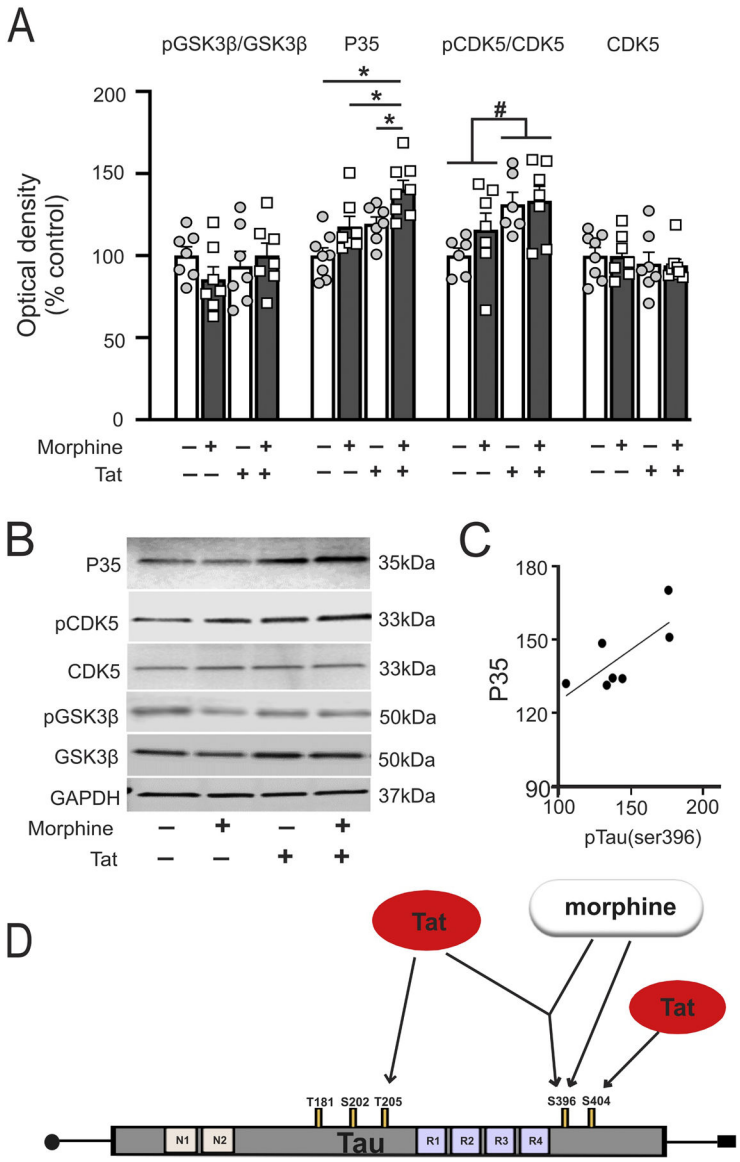

Fig. 5.

Striatal GSK3β, CDK5 and p35 levels. (**A**) p35, the coactivator of CDK5 was increased in the striatum of morphine-treated HIV-1 Tat transgenic mice as compared to all other treatment groups. Phosphorylated CDK5 was increased in the striatum of Tat transgenic mice irrespective of treatment. There were no significant differences in any of the evaluated groups for total CDK5 and GSK3β levels by two-way ANOVA. (**B**) Representative immunoblot images for p35, CDK5, GSK3β, and GAPDH. (**C**) Pearson correlation revealed that p35 level in morphine-treated Tat transgenic mice positively correlated with pSer396 levels. (**D**) Tat and morphine dependent hyperphosphorylation of tau differs among brain regions. Moreover, Tat and morphine appear to differentially (and perhaps synergistically) phosphorylate separate pathological tau domains. Morphine may preferentially phosphorylate Ser395, while Tat may selectively phosphorylate Thr205 and Ser404. The tauopathy induced by Tat and morphine is analogous to pathological changes accompanying

accelerated brain aging. Data are expressed as mean ± SEM. # indicates significant main effects by two-way ANOVA. * indicates planned contrasts that showed differences with Tukey's *post hoc* test ($p < 0.05$). p: phosphorylated tau, Ser: serine, Thr: threonine. n = 6–8/group.